Indian J. pure appl. Math., 34(6) : 819-830, June 2003

TRANSVERSE VIBRATION OF POLAR ORTHOTROPIC PARABOLICALLY TAPERED CIRCULAR PLATES

A. H. ANSARI AND U. S. GUPTA

Department of Mathematics, Indian Institute of Technology, Roorkee 247 667, India

(*Received* 29 *March* 2000; *after final revision* 28 *November* 2000; *accepted* 30 *April* 2003)

Forced axi-symmetric vibrations of polar orthotropic parabolically tapered circular plates are discussed on the basis of classical plate theory. Ritz method has been employed to obtain the solution. The deflection function and the bending moments for forced vibrations of the plate are presented for various values of taper parameter, flexibility parameter and rigidity ratio. A comparison of results with those available in literature shows an excellent agreement.

Key Words: Forced Axi-symmetric Vibration; Polar Orthotropy, Natural Frequency; Classical Plate Theory

1. INTRODUCTION

A considerable amount of work has been done on forced vibrations of isotropic plates of various geometry such as circular, annular, rectangular, polygonal etc. and is reported[2-34]. When plates are used in operations they are often subjected to symmetric transverse loads. The stability of structural components exposed to air flow is one of the major consideration in the fabrication of aerospace structures, where high speed air flow is encountered. Thus the study of dynamic behaviour of plates with loads is essential. The forced vibration of plates has been studied by Leissa[2-4]. Liew[5] studied the effect of various types of geometry on forced vibration of isotropic plates. An exhaustive work on forced vibrations of isotropic plates has been done by Laura *et al.*[6-16]. Laura *et al.*[13-16] analysed the dynamic behaviour of isotropic circular plates of variable thickness with elastically restrained edge. The analysis of vibration of plates with edges elastically restrained against translation and rotation is an important problem in aeronautical and naval structural engineering. In aircraft structures, the individual plates are connected to the other plates or stiffeners at their boundaries and thus have elastic restraint at their edges[6-16]. Some recent researches on forced vibration of plates are presented by Weisensel and Schlack[23-24] and Gupta and Goel[27]. Most of these studies deal with forced axisymmetric vibration of isotropic plates. Conventional metals are being replaced by fibre-reinforced composite materials in various structural components, as they possess desired stiffness, strength and light weight characteristics. The analysis of plates exhibiting anisotropy has received greater attention to increasing use of fibre-reinforced materials, especially in aerospace industries. Non-uniform plates are used to achieve a better distribution to strength and weight to satisfy architectural functional requirements. In case of orthotropic plates, the forced response depends on the rigidity ratio (Lekhnitskii[31], pp. 372). The problem is of interest due to its use in the design of transducers.

The present study is concerned with the forced axi-symmetric vibrations of polar orthotropic plates of parabolically varying thickness with elastically restrained edge subjected to uniformly distributed loads.

2. ENERGY EXPRESSION

Consider a thin circular plate of radius a, thickness $h = h(r)$, elastically restrained against translation and rotation and subjected to $P(r) \cos \omega t$ type of excitation extending from $r = r_0$ to $r = r_1$. Let

(r, θ) be the polar co-ordinates of any point on neutral surface of the plate referred to the centre of the plate as origin (Figure 1).

The maximum kinetic energy of the plate is given by

$$T_{\max} = \frac{1}{2} \rho \omega^2 \int_0^a \int_0^{2\pi} h w^2 \, r d\theta \, dr \qquad \dots (1)$$

where w is the transverse deflection, ρ the mass density and ω the frequency in radians per second.

The maximum strain energy of the plate is given by

$$U_{\max} = \frac{1}{2} \int_0^a \int_0^{2\pi} \left[D_r \left\{ \left(\frac{\partial^2 w}{\partial r^2} \right)^2 + 2 \upsilon_\theta \frac{\partial^2 w}{\partial r^2} \left(\frac{1}{r} \frac{\partial w}{\partial r} \right) \right\} + D_\theta \left(\frac{1}{r} \frac{\partial w}{\partial r} \right)^2 \right] r \, dr d\theta$$

$$+ \frac{1}{2} ak \int_0^{2\pi} w^2 (a, \theta) \, d\theta + \frac{1}{2} ak_\phi \int_0^{2\pi} \left(\frac{\partial w (a, \theta)}{\partial r} \right)^2 d\theta \qquad \dots (2)$$

where k and $1/k_\phi$ are the translational and rotational flexibilities of the springs and $D_r(r) = E_r h^3/12(1 - v_\theta v_r)$, $D_\theta(r) = E_\theta h^3/12(1 - v_\theta v_r)$ are the flexural rigidities of the plate.

The work done by external force $P(r)$ acting on the plate in the direction parallel to z-axis is given by

$$V_{\max} = \int_0^{2\pi} d\theta \int_{r_0}^{r_1} w P(r) \, r dr \qquad \dots (3)$$

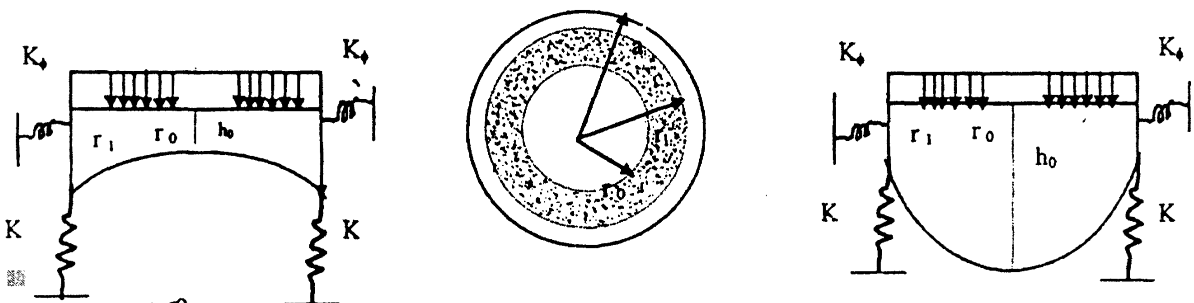

FIG. 1

3. METHOD OF SOLUTION : RITZ METHOD

Ritz method requires that the functional

$$J(w) = U_{\max} - V_{\max} - T_{\max} = \frac{1}{2} \int_0^a \int_0^{2\pi} \left[D_r \left\{ \left(\frac{\partial^2 w}{\partial r^2} \right)^2 + 2 \upsilon_\theta \frac{\partial^2 w}{\partial r^2} \left(\frac{1}{r} \frac{\partial w}{\partial r} \right) \right\} \right.$$

$$+ D_\theta\left(\frac{1}{r}\frac{\partial w}{\partial r}\right)^2\Bigg] r\,dr\,d\theta$$

$$+ \frac{1}{2} ak \int_0^{2\pi} w^2(a,\theta)\,d\theta + \frac{1}{2} ak_\phi \int_0^{2\pi}\left(\frac{\partial w(a,\theta)}{\partial r}\right)^2 d\theta$$

$$-\int_0^{2\pi} d\theta \int_{r_0}^{r_1} w\,P(r)\,r dr - \frac{1}{2}\rho\,\omega^2 \int_0^a \int_0^{2\pi} h\,w^2\,r d\theta\,dr \qquad \dots (4)$$

be minimised.

For a uniformly distributed load P_0 extending from $r = r_0$ to $r = r_1$ we have

$$P(r) = q_0 = \frac{P_0}{\pi(r_1^2 - r_0^2)}[U(r - r_0) - U(r - r_1)].$$

Introduce the non-dimensional variables $W = w/(a^4 q_0/D_{r0})$, $R = r/a$, $R_0 = r_0/a$, $R_1 = r_1/a$ and assume the deflection function as

$$W(R) = \sum_0^m A_i W_i(R) = \sum_1^m A_i(1 + \alpha_i R^4 + \beta_i R^{1+p})\,R^{2(i-1)} \qquad \dots (5)$$

where A_i are undetermined coefficients, $p^2 = E_\theta/E_r$ and α_i, β_i are unknown constants to be determined from the boundary conditions

$$K_\phi \frac{dW_i}{dR}\Bigg|_{R=1} = -(1-\alpha)^3\left[\frac{d^2 W_i}{dR^2} + \upsilon_\theta\left(\frac{1}{R}\frac{dW_i}{dR}\right)\right]_{R=1} \qquad \dots (6)$$

$$KW_i(1) = (1-\alpha)^3\left[\frac{d}{dR}\left(\frac{d^2 W_i}{dR^2} + \frac{1}{R}\frac{dW_i}{dR}\right) - \frac{1}{2}D_{k0}\left(\frac{1}{R}\frac{dW_i}{dR} - \frac{W_i}{R^2}\right)\right]_{R=1} \qquad \dots (7)$$

The unknown constants α_i and β_i are determined using these boundary conditions which give

$$\alpha_i = \frac{t_{12i}\,t_{23i} - t_{13i}\,t_{22i}}{t_{11i}\,t_{22i} - t_{12i}\,t_{21i}},\ \beta_1 = \frac{t_{21i}\,t_{13i} - t_{23i}\,t_{11i}}{t_{11i}\,t_{22i} - t_{12i}\,t_{21i}} \qquad \dots (8)$$

where $t_{11i} = K_\phi(2i+2) + (1-\alpha)^3((2i+2)(2i+1) + \upsilon_\theta(2i+2))$

$t_{12i} = K_\phi(2i+p-1) + (1-\alpha)^3((2i+p-1)(2i+p-2) + \upsilon_\theta(2i+p-1))$

$t_{13i} = K_\phi(2i-2) + (1-\alpha)^3((2i-2)(2i-3) + \upsilon_\theta(2i-2))$

$t_{21i} = K - (1-\alpha)^3((2i+2)(2i+1)^2 - (2i+2) - 0.5\,D_{k0}(2i+1))$

$$t_{22\,i} = K - (1-\alpha)^3\,((2i+p-1)(2i+p-2)^2 - (2i+p-1) - 0.5\,D_{k0}\,(2i+p-2))$$

$$st_{23\,i} = K - (1-\alpha)^3\,((2i-2)(2i-3)^2 - (2i-2) - 0.5\,D_{k0}\,(2i-3))$$

where $$K = \frac{a^3 k}{D_{r0}},\ K_{\Phi} = \frac{ak_{\Phi}}{D_{r0}},\ D_{k0} = \frac{D_k}{D_{r0}}.$$

The functional $J(w)$ given by (4), on introduction of non-dimensional variables and using relation (5) becomes

$$J(W) = \pi D_{r0}\left[\int_0^1 \left[(1-\alpha R^2)^3\left\{\left(\frac{d^2 W}{dR^2}\right)^2 + 2\,\upsilon_\theta \frac{d^2 W}{dR^2}\left(\frac{1}{R}\frac{dW}{dR}\right)\right\} + p^2\left(\frac{1}{R}\frac{dW}{dR}\right)^2\right] R\,dR + KW^2(1) + K_\phi\left(\frac{dW}{dR}\right)^2_{R=1} - \int_{R_0}^{R_1} 2\,w\,1(R)\,R\,dR - \Omega^2\int_0^1 (1-\alpha R^2)\,W^2\,R\,dR\right] \quad \ldots (9)$$

where $h = h_0(1-\alpha R^2)$ specifies the parabolic thickness variations, h_0 being thickness of the plate at the centre, α the taper parameter and $D_{r0} = E_r h_0^3/12(1-\nu_\theta \nu_r)$, $\Omega^2 = a^4 \rho\,\omega^2 h_0/D_{r0}$.

The minimization of the functional $J(W)$ given by (9) requires

$$\frac{\partial J(W)}{\partial A_i} = 0,\ i = 1, \ldots, m \quad \ldots (10)$$

This leads to a system of non-homogeneous equations in A_j,

$$(a_{ij} - \Omega^2 b_{ij})\,A_j = C_i \quad i, j = 1\ldots, m \quad \ldots (11)$$

where $$a_{ij} = \int_0^1 (1-\alpha R^2)^3\left[W_i'' W_j'' + 2\,\upsilon_\theta W_i''\left(\frac{W_j'}{R}\right) + p^2\left(\frac{W_i'}{R}\right)\left(\frac{W_j'}{R}\right)\right] R\,dR + KW_i(1)\,W_j(1) + K_\phi W_i'(1)\,W_j'(1) \quad \ldots (12)$$

$$b_{ij} = \int_0^1 (1-\alpha R^2)\,W_i W_j R\,dR \quad \ldots (13)$$

and $$C_i = \int_{R_0}^{R_1} 2\,W_i R\,dR. \quad \ldots (14)$$

The solution of the system of eqs. (10) gives the values A_i. Hence the transverse deflection W and the radial and tangential bending moments

$$\frac{M_r}{q_0 a^2} = -(1-\alpha R^2)^3 \left[\frac{d^2 W}{dR^2} + \nu_\theta \frac{1}{R}\frac{dW}{dR} \right] \quad \text{... (15)}$$

$$\frac{M_\theta}{a^2 q_0} = (1-\alpha R^2)^3 \left[\nu_r \frac{d^2 W}{dR^2} + p^2 \frac{1}{R}\frac{dW}{dR} \right] \quad \text{... (16)}$$

are computed.

4. Numerical Results

Numerical results have been calculated for transverse vibration of polar orthotropic plates of parabolically varying thickness for different values of taper parameter $\alpha (= 0; \pm 0.3)$, rigidity ratio E_θ/E_r (= 1.00, 2.00, 5.00) and flexibility parameter $K_\phi (= 0, 10, 10^{20} \equiv \infty)$. The natural frequencies for free vibrations are obtained by putting $P(r) = 0$. In case of forced vibration the non-dimensional frequency parameter is taken as $\Omega = \eta\, \Omega_{00}$ for $\Omega < \Omega_{00}$ and $\Omega = \Omega_{00} + \eta\,(\Omega_{01} - \Omega_{00})$ for $\Omega_{00} < \Omega < \Omega_{01}$. The normalized deflection and bending moments are obtained for $\eta = 0.2$, Poisson's ratio ν_θ of the plate being fixed as 0.3.

5. Discussion

In case of forced vibrational problems, the deflection and bending moments are of great interest from the design point of view. The results are presented graphically for transverse deflection and bending moments (radial as well as tangential) for various values of plate parameters i.e. E_θ/E_r (= 1.0, 2.0, 5.0), $\alpha = \pm 0.3$), $k\phi$ = (0.0, 1.0, 20, ∞) $\eta = 0.2$ for simply supported and clamped plates. The radial and tangential bending moments at the centre of the plate ($R = 0$) are zero for orthotropic plates, whereas they are non-zero in case of isotropic plates. For other values of radial co-ordinate R, the bending moments are found to be dependent on the orthotropic nature of the plate i.e. whether the plate is radially stiffened ($E_\theta < E_r$) or circumferentially stiffened ($E_\theta > E_r$). Numerical results for radial bending moment $M_r/q_0 a^2$ and tangential bending moment $M_\theta/q_0 a^2$ are given for circumferentially stiffened plates only because in case of radially stiffened plate ($E_\theta < E_r$) infinite stress is developed at the centre. The results for deflection and bending moments are presented for different types of loadings:

(*i*) when the load is distributed uniformly on the disk extending from $R_0 = 0$ to $R_1 = 0.5$, presented in figures 2(*a-b*) – 4(*a-b*) for $\Omega < \Omega_{00}$ and $\Omega_{00} < \Omega < \Omega_{01}$,

(*ii*) when the load is distributed uniformly over the annular region extending from $R_0 = 0.3$ to $R_1 = 0.7$, presented in figures 5(*a-b*) - 7(*a-b*) for $\Omega < \Omega_{00}$ and $\Omega_{00} < \Omega < \Omega_{01}$,

(*iii*) when the load is distributed uniformly over the entire plate, presented in figures, 8(*a-b*) 10(*a-b*) for $\Omega < \Omega_{00}$ and $\Omega_{00} < \Omega < \Omega_{01}$, the total load on the plate being constant for all the cases.

Figures 2(*a*, *b*) –4(*a*, *b*) present the transverse deflection and bending moments (radial as well as tangential) for simply supported (SS, i.e. $K_\phi = 0, K = 10^{20}$), ($K_\phi = 10, K = 10^{20}$) and clamped edge (*C*1) for $K_\phi = 10^{20}, K = 10^{20}$) conditions for disk loaded plate at different points along the radius of the plates for $\Omega < \Omega_{00}$ and $\Omega_{00} < \Omega < \Omega_{01}$ respectively. The taper parameter α has been taken as ($= \pm 0.3$). The deflection is observed to be maximum at the centre. Further, the deflection function decreases as the flexibility parameter K_ϕ increases for $\Omega < \Omega_{00}$ as well as for $\Omega_{00} < \Omega < \Omega_{01}$. The deflection for a simply supported plate is always greater than that for a clamped edge plate, other plate parameters being fixed. Figure also demonstrates that the deflection for a centrally thinner plate ($\alpha = -0.3$) is less than that for a centrally thicker plate ($\alpha = 0.3$) for all boundary conditions, reason being greater mass attribution for $\alpha = -0.3$ than that for α = 0.3. The transverse deflection $W/a^4 q_0 D_{r0}$ at the centre is more pronounced for $\alpha = 0.3$ for a simply supported plate. Figures 3(*a-b*) present the radial bending moments $M_r q_0 a^2$ for plates when $\Omega < \Omega_{00}$ and $\Omega_{00} < \Omega < \Omega_{01}$. The moment at the edge for simply supported plate is zero, and is found to increase with the increase in K_ϕ. The peak of radial bending moment of simply supported plate lies to the right of R = 0.3, but as K_ϕ. increases, they shift towards the origin. The peak of the tangential bending moment $M_\theta/q_0 a^2$ (Figures 4(*a-b*)) is greater than that for the radial bending moment (Figures 3(*a-b*)) measured from the mid-surface. Figures 5(*a-b*) – 7(*a-b*) present the deflections and bending moments for annular loading. The transverse deflection for such a plate is greater than that for a disk loaded plate (Figures 2(*a-b*)) for the corresponding values of plate parameters. In case of uniformly loaded plate (Figure 8(*a-b*) – 10(*a-b*)), the deflection function and bending moments attain the maximum value as compared to the disk and annular loaded plates. The radial and tangential bending moments for disk loading are observed to be greater than that for a annular loading but less than that for a uniformly loaded plate Figures (3(*a-b*) – 4(*a-b*), 6(*a-b*) – 7(*a-b*), 9(*a-b*) – 10(*a-b*)).

Table I depicts the transverse deflection $W/a^4 q_0 D_{r0}$ at the centre for different values of rigidity ratio E_θ/E_r, taper parameter, flexibility parameter and types of loading. The transverse deflection decreases as the flexibility parameter K_ϕ increases. Further it can be observed that the transverse deflection decreases as the rigidity ratio E_θ/E_r increases, whatever be the other plate parameters.

A comparison of results for the deflection and bending moments for simply supported and clamped plates obtained by Laura *et al.*[13] using Galerkin's method for uniformly loaded plate of uniform thickness is presented in figure 11 for $\Omega/\Omega_{00} = 0.7$. Figure shows that the results are in excellent agreement. Table II compares the results well with those of Laura *et al.*[13]. A comparison of results with those of Laura *et al.*[16] using Ritz method, which employs polynomial co-ordinate functions is presented in Table III.

TABLE I : The amplitude of dimensionless displacement $W/a^4 q_0 D_{r0}$ at the centre as a function of rigidity ratio E_θ/E_r, taper α, flexibility parameter K_ϕ and loadings for $K = 10^{20}$

K_ϕ		Rigidity ratio $E_\theta/E_r = 2.0$				Rigidity ratio $E_\theta/E_r = 5.0$			
		$\Omega < \Omega_{00}$		$\Omega_{00} < \Omega < \Omega_{01}$		$\Omega < \Omega_{00}$		$\Omega_{00} < \Omega < \Omega_{01}$	
		$\alpha = -0.3$	$\alpha = 0.3$	$\alpha = -0.3$	$\alpha = 0.3$	$\alpha = -0.3$	$\alpha = 0.3$	$\alpha = -0.3$	$\alpha = 0.3$
0.0	Ω	1.4043	1.0587	12.8853	10.0724	2.0210	1.4064	16.7993	12.5771
	Disk	0.014645	0.026825	–0.005184	–0.008765	0.006563	0.013886	–0.002844	–0.005299
	Annular	0.017202	0.033299	–0.007622	–0.013116	0.007820	0.017816	–0.004626	-0.008259
	Uniform	0.029817	0.057858	–0.012924	–0.022821	0.013521	0.031014	–0.007883	-0.014540
10.0	Ω	2.1882	1.6880	16.9782	13.7796	2.7288	2.0565	20.5952	16.4469
	Disk	0.007396	0.012955	–0.004491	–0.006815	0.004264	0.007830	–0.002770	–0.004311
	Annular	0.007595	0.014124	–0.006036	–0.009302	0.004586	0.009014	–0.003933	–0.006210
	Uniform	0.12919	0.023306	–0.009771	–0.014910	0.007730	0.014798	–0.006386	-0.010025
10^{20}	Ω	2.7669	1.8185	20.8602	14.7473	3.3760	2.2120	24.9113	17.5794
	Disk	0.005400	0.011661	0.003801	–0.006333	0.003245	0.007079	–0.002402	–0.004022
	Annular	0.004944	0.012333	–0.004591	–0.008419	0.003150	0.007922	–0.003093	-0.005655
	Uniform	0.008253	0.020076	–0.006999	–0.013143	0.005159	0.012784	–0.004683	-0.008858

TABLE II : Comparison of displacement $W/a^4 q_0 D_{r0}$ for simply supported circular plate of linearly varying thickness for $\nu_\theta = 0.25$

α	Ref [13]	Present
–0.5708	0.1817	0.1815
0.0	0.06568	0.0656
–0.33333	0.1143	0.1127

TABLE III : Comparison of amplitude of dimensionless displacement and radial bending moment at the centre as a function of $\Omega (= \Omega < \Omega_{00})$ and $(= \Omega_{00} < \Omega < \Omega_{01})$ for uniform isotropic plates

		$\Omega < \Omega_{00}$				$\Omega_{00} < \Omega < \Omega_{01}$			
		$W/a^4 q_0 D_{r0}$		$M_r/a^2 q_0$		$W/a^4 q_0 D_{r0}$		$M_r/a^2 q_0$	
$K_\phi = \infty$	η	Ref [16]	present	Ref [16]	Present	Ref [16]	Present	Ref [16]	Present
$\Omega_{00} = 10.215$	0.2	0.01630	0.01630	0.085	0.08524	0.011	0.01181	0.084	0.08468
	0.4	0.01872	0.01872	0.099	0.09952	0.0055	0.00553	0.051	0.05121
$\Omega_{01} = 39.771$	0.6	0.02479	0.02479	0.135	0.13533	0.0040	0.0040	0.0388	00.03840
	0.8	0.04461	0.04461	0.253	0.25281	0.0044	0.00446	0.080	0.08001
$K_\phi = 0$	0.2	0.06640	0.06640	0.215	0.21554	0.0226	0.02263	0.094	0.09407
$\Omega_{00} = 4.9351$	0.4	0.07603	0.07603	0.248	0.24874	0.0094	0.00946	0.052	0.05224
	0.6	0.10010	0.10010	0.331	0.33179	0.0062	0.006238	0.049	0.04948
$\Omega_{01} = 29.721$	0.8	0.17875	0.17877	0.603	0.60332	0.0063	0.006329	0.076	0.07653

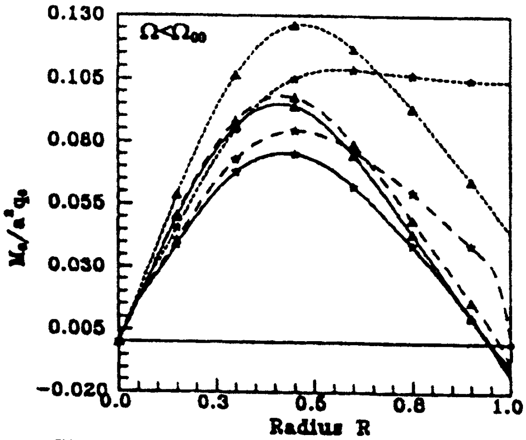

Fig. 4(a) Tangential bending moment

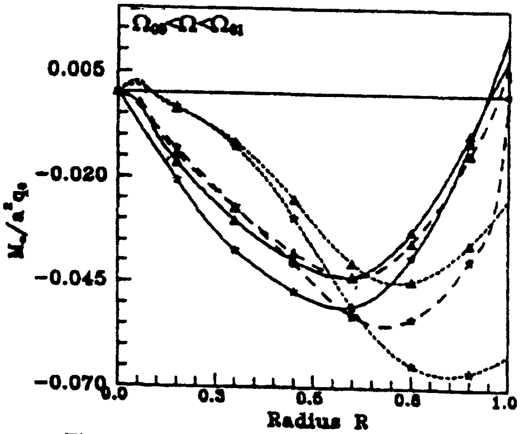

Fig. 4(b) Tangential bending moment

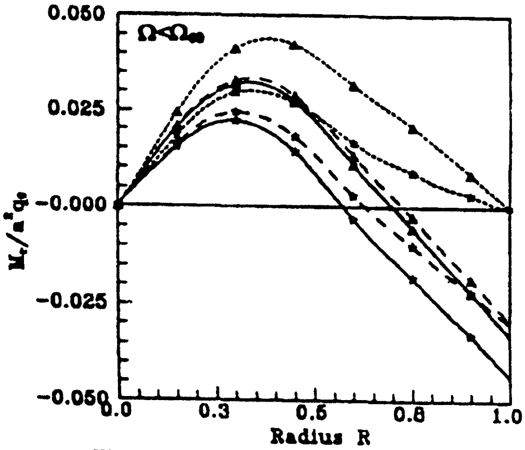

Fig. 3(a) Radial bending moment

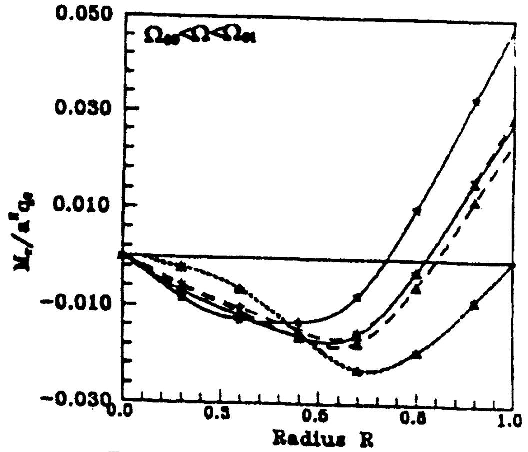

Fig. 3(b) Radial bending moment

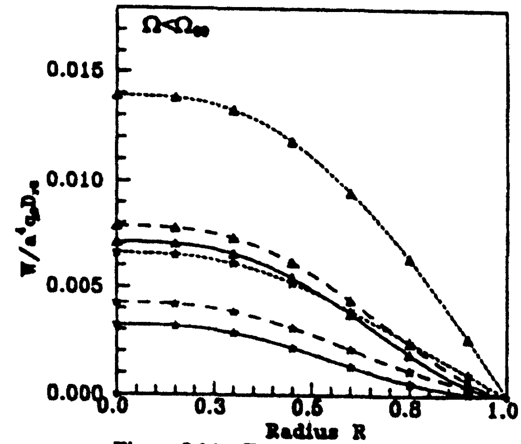

Fig. 2(a) Transverse deflection

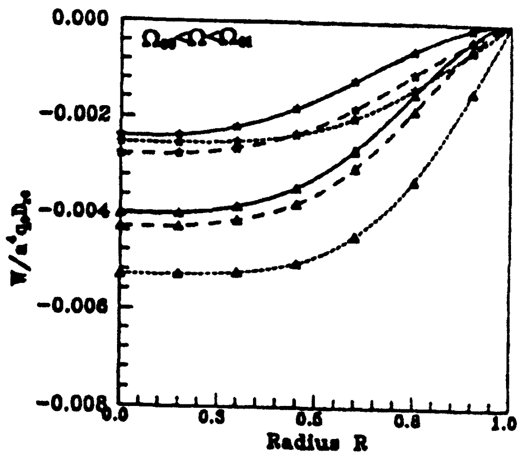

Fig. 2(b) Transverse deflection

FIGS. 2-4. Disk loading for $K_\phi = 0.0$ (SS): --------, $K_\phi = 10$: - - - - -, $K_\phi = 10^{20}$ (CL):______ $\nu_\theta = 0.3, E_\theta/E_r = 5.0$.
Keys PVT plates $\alpha = -0.3$; ***; $\alpha = 0.3$: ▲▲▲

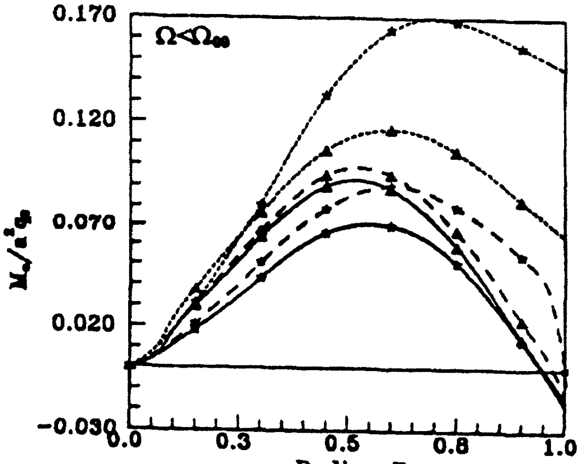

Fig. 7(a) Tangential bending moment

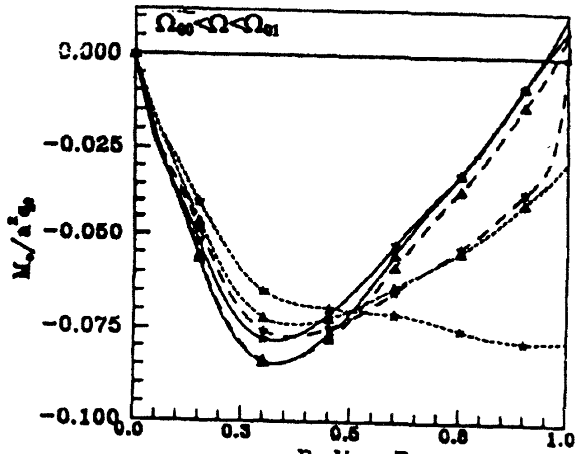

Fig. 7(b) Tangential bending moment

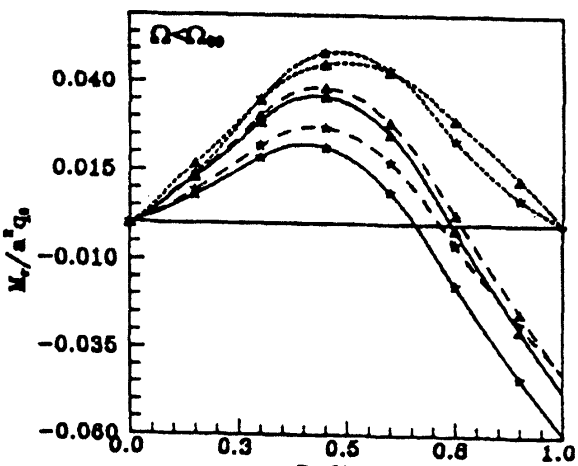

Fig. 6(a) Radial bending moment

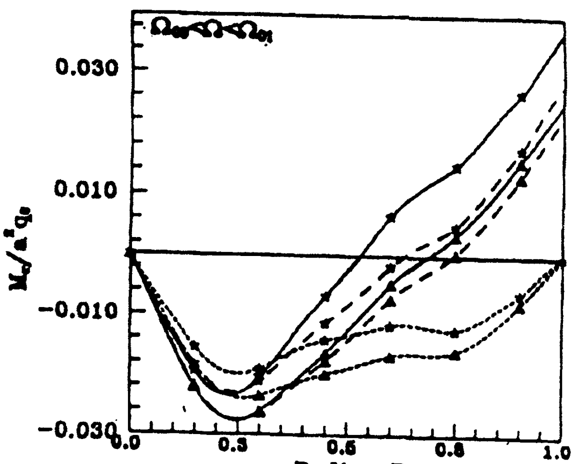

Fig. 6(b) Radial bending moment

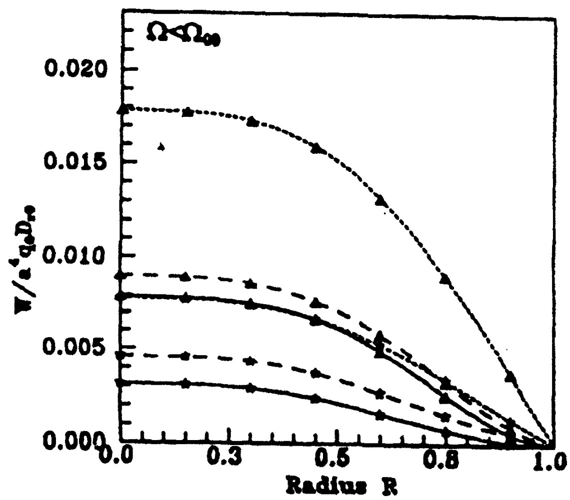

Fig. 5(a) Transverse deflection

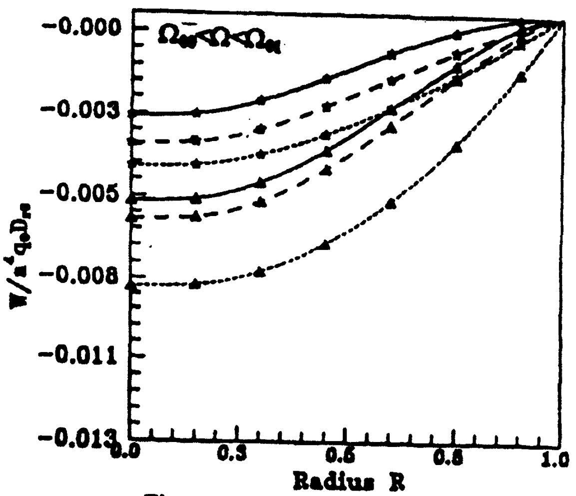

Fig. 5(b) Transverse deflection

FIGS. 5-7. Annular loading for K_ϕ = 0.0 (SS): --------, K_ϕ = 10: - - - - -, $K_\phi = 10^{20}$ (CL):_____ $\nu_\theta = 0.3$, E_θ/E_r = 5.0. Keys PVT plates $\alpha = -0.3$; ***; α = 0.3: ▲▲▲

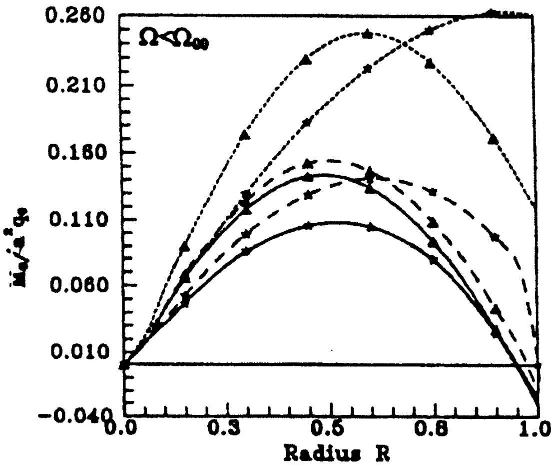

Fig. 10(a) Tangential bending moment

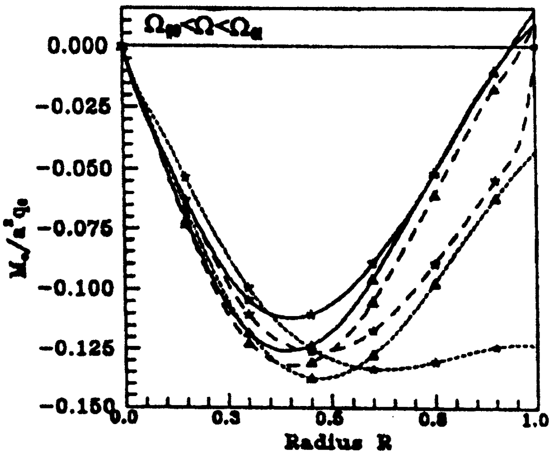

Fig. 10(b) Tangential bending moment

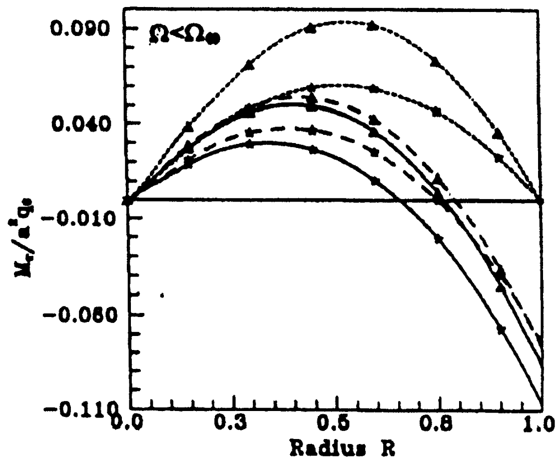

Fig. 9(a) Radial bending moment

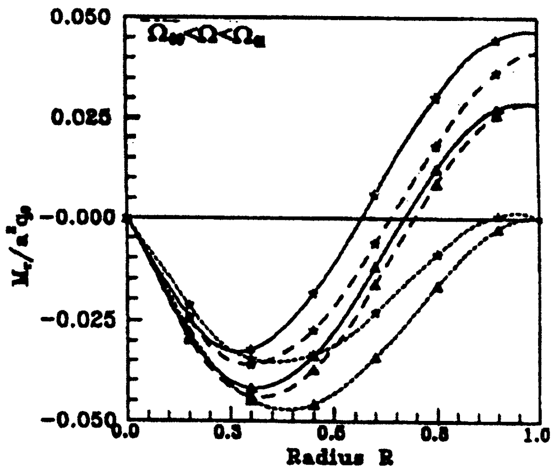

Fig. 9(b) Radial bending moment

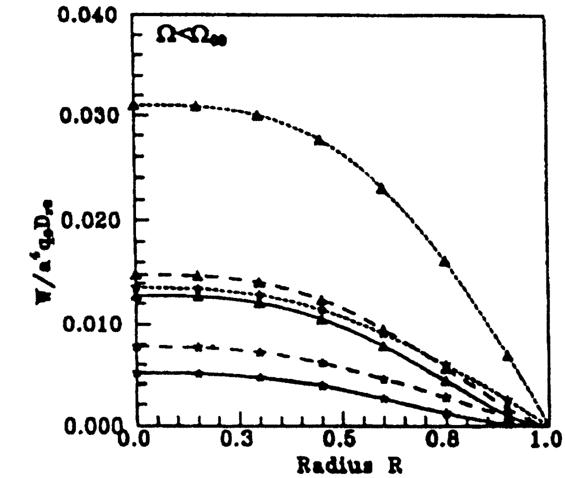

Fig. 8(a) Transverse deflection

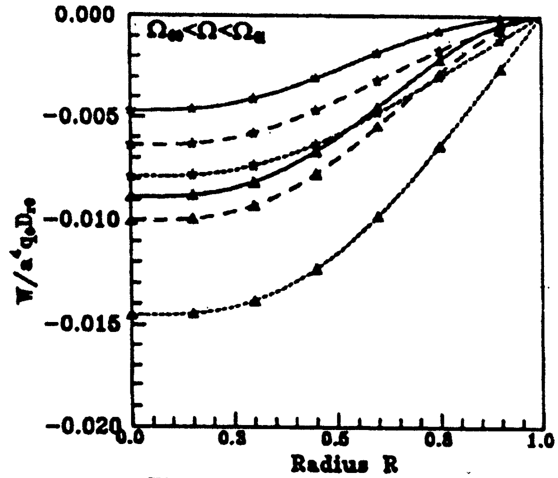

Fig. 8(b) Transverse deflection

FIGS. 8-10. Uniform loading fork $K_\phi = 0.0$ (SS): --------, $K_\phi = 10$: - - - - -, $K_\phi = 10^{20}$ (CL):_____ $\nu_\theta = 0.3$, $E_\theta/E_r = 5.0$. Keys PVT plates $\alpha = -0.3$; ***; $\alpha = 0.3$: ▲▲▲

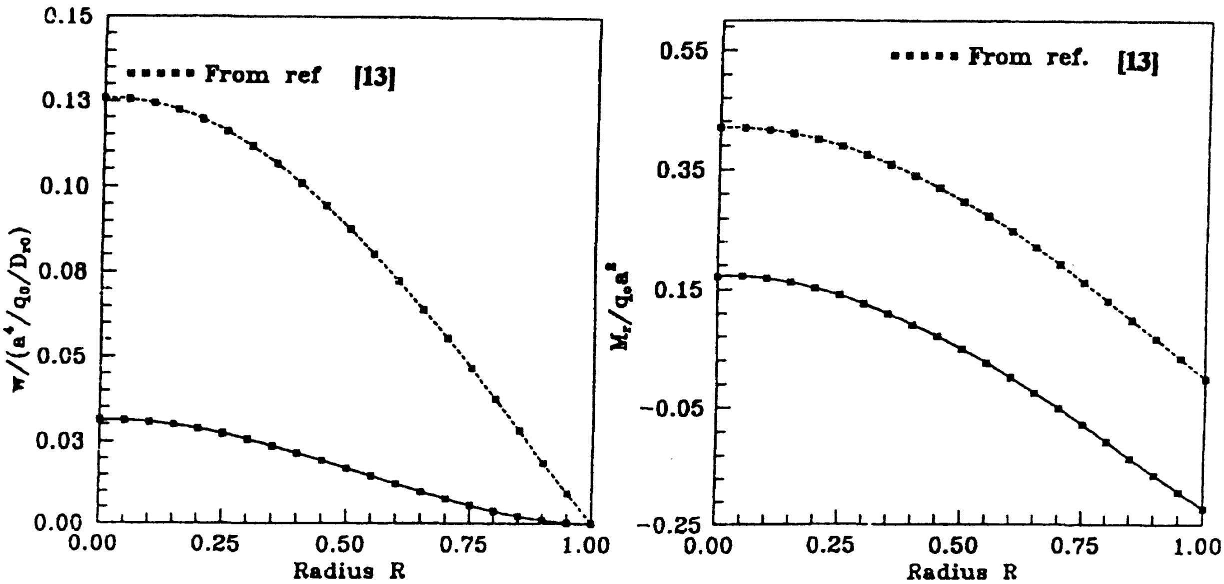

FIG. 11. Deflection and bending moment for $K_\phi = 0$ (*SS*): ----- and $K_\phi = 10^{20}$ (CI): ——

6. CONCLUSION

The present work analyses the forced vibrations of polar orthotropic plates of parabolically varying thickness on the basis of classical plate theory. Ritz method has been employed to obtain the solution. Natural frequencies are obtained by putting $P(r) = 0$. The deflection function and bending moment are presented for different values of flexibility parameter K_ϕ, taper parameter α and rigidity ratio E_θ/E_r. Transverse deflection for a circumferentially stiffened plate decreases with the increase in rigidity ratio as well as flexibility parameter K_ϕ, keeping the flexibility parameter of the translational spring $K = 10^{20}$. Thus the transverse deflection for simply supported plate is greater than that for a clamped plate. Numerical results presented in figures show that radial bending moment for simply supported plate at the edge is zero but it increases with the increase in flexibility parameter K_ϕ. The transverse deflection for, $\alpha = -0.3$ is less than that for $\alpha = 0.3$. The reason being greater mass attribution for $\alpha = -0.3$, keeping other plate parameters fixed. The transverse deflection and bending moments for uniformly loaded plate are greater than that for disk and annular loaded plates.

REFERENCES

1. A. W. Leissa, *Vibration of plates*, NASA SP-160, (1969), U.S. Washington
2. A. W. Leissa. *J Sound and vibration* **56**, (1978), 313.
3. A. W. Leissa. *J. Sound and vibration*, **134** (1989), 435.
4. A. W. Leissa and Y. T. Chern. *J. Vibration and Acoustics*, **114** (1992), 106.
5. K. M. Liew, *Applied Mechanics*, ASCE (1992), **118**, 1783-89. Response of plates of arbitrary shape subjected to static loading
6. P. A. A. Laura, L. E. Luisoni and J. J. Lopez. *J sound and Vibration* **47(2)** (1976), 287-91.
7. P. A. A. Laura, J. L. Pombo and L. E. Luisoni. *J. sound and Vibration*, **45(2)** (1976), 225-35
8. D. V. Bambill, P. A. A. Laura and E. Romanelli, *Ocean Engineering* **14** (1987), 527.
9. C. Filipich, P. A. A. Laura, M. Sonemblum and E. Gil. *J. Sound and Vibration*, **126** (1988) 1.
10. P. A. A. Laura, B. V. Greco de, J. C. Utjes and R. Carnicer. *J. Sound and Vibration*, **120** (1988), 587.
11. P. A. A. Laura and R. Duran, *J. Sound and Vibration*, **42**: (1975) 129.
12. E. A. Susemihl and P. A. A. Laura, *J. Ship Research*, **V-14**: (1977) 24-28.

13. P. A. A. Laura, C. Filipich and R. D. Santos, *J. Sound and Vibration*, **52(2)** (1977), 243-51.
14. C. Filipich, P. A. A. Laura and R. D. Santos, *J. Sound and Vibration*, **50** (1977), 445.
15. B. V. de Greco and P. A. A. Laura, *J. Sound and Vibration*, **94** (1984), 525.
16. P. A. A. Laura, D. R. Avalos, H. A. Larrondo, *J. Sound and Vibration*, **136(1)** (1990), 146-50.
17. H. Reismann, *J. Applied Mechanics*, **26** (1959), 526.
18. H. Reismann, *J. Applied Mechanics*, **35** (1968), 510.
19. B. K. Donaldson, *J. Sound and Vibration*, **30(4)**: 397-417.
20. P. B. Beaudan and H. Reismann, *J. Applied Mechanics*, **54** (1987), 472.
21. K. Chandrasekharan and V. X. Kunukkasseril, *J. Sound and Vibration*, **44**: 407.
22. E. de Langre, F. Axisa and D. Guibaud, *In*: Eds. C. A. Brebbia and A. C. Mirander, *Proceedings of International Boundary Element Symposium*, Nice, France, 15-17 May 1990.
23. G. N. Weisensel and A. L. Schlack, *J. Applied Mechanics*, **60** (1993), 649.
24. G. N. Weisensel and A. L. Schlack, *J. Analytical and experimental model analysis*, **5**: 239.
25. R. S. Weiner, *J. Applied Mechanics*, **32** (1965), 893.
26. P. K. Roy and N. Ganesan, *Computer and Structures*, **45** (1992), 593.
27. A. P. Gupta and N. Goel, *J. Mechanical Sciences* **36(5)** (1994), 439-48.
28. Ramalingeswara, S. Rao and N. Ganesan, *J. Sound and Vibration*, (1994), 737-46.
29. S. P. Timoshenko and S. Woinowsky-Krieger, Theory of plates and shells McGraw-Hill, New York, N.Y., 1959.
30. W. Nowacki, Dynamics of elastic systems, New York : John Wiley and Sons, 1960.
31. S. G. Lekhnitskii, "Anisotropic plates", Breach Science Publishers Inc., New York, 1985.
32. M. Mukhopadhyay, *Ocean Engineering*, V-**8**, No. 5 (1981), 497-505.
33. A.H. Sheikh and M. Mukhopadhyay, *Int. J. Series C*, **V-36, 3** (1993), 301-306.
34. G. Sinha and M. mukhopadyay, *Vibration and Acoustics*, **V-117/1**, (1995), 11-16.